CHAPTER IV
RESULTS AND DISCUSSION

4.1. Catalyst Preparation

Pt/KL catalysts were prepared by two mothod, *i.e.*, IWI and VPI methods, and the results were presented in Table 4.1. In addition, the result of Pt/SiO_2 prepared by IWI method was also presented in Table 4.1 as well.

All catalysts were labeled with a two-digit system in order to systematize all the prepared catalysts. No.00 represents the reference catalyst, Pt/SiO_2. The first digit denotes the catalyst preparation method, while the second digit denotes the particular promoter added to that catalyst. For the first digit, 1 stands for IWI method and 2 stands for VPI method. For the second digit, 1 stands for no promoter added to that catalyst while 2, 3, and 4 stand for Ce, Er, and Yb promoters added to the catalyst respectively. All promoted catalysts were designed with 1.5 wt% rare earth (RE).

4.2. Catalyst Characterization

The catalysts were characterized by two methods: (i) BET surface area analysis, and (ii) atomic absorption spectroscopy (AAS).

4.2.1. BET Surface Area Analysis

BET surface area analysis was used to verify the surface area and pore volume of the catalysts. The BET characterization results were shown in Tables 4.2 and 4.3.

Table 4.1 Pt/SiO_2 & Pt/KL catalyst preparation results prepared by both VPI & IWI mothod.

Sample number	Catalyst name	Preparation method	Pt solution	RE solution	RE content (wt%)	Finished catalyst (gram)
00	Pt/SiO_2	IWI	1*	-	0.00	2.7300
00A	Pt/SiO_2	IWI	1	-	0.00	4.4878
11	Pt/KL	IWI	1	-	0.00	2.3675
11A	Pt/KL	IWI	1	-	0.00	3.0817
11B	Pt/KL	IWI	1	-	0.00	3.8777
12	Pt/CeKL	IWI	1	2†	0.15	1.9539
13	Pt/ErKL	IWI	1	3‡	0.15	2.7945
14	Pt/YbKL	IWI	1	4§	0.15	2.4267
21	Pt/KL	VPI	5**	-	0.00	N/A
22	Pt/CeKL	VPI	5	6††	0.15	2.3920
23	Pt/ErKL	VPI	5	7‡‡	0.15	2.4350
24	Pt/YbKL	VPI	5	8§§	0.15	N/A

* Pt solution: 1 = Tetraammine platinum (II) nitrate
† RE solution: 2 = Cerium (III) nitrate hexahydrate
‡ RE solution: 3 = Erbium (III) nitrate pentahydrate
§ RE solution: 4 = Ytterbium (III) nitrate pentahydrate
** Pt solution: 5 = Platinum (II) acetyl-acetonate
†† RE solution: 6 = Cerium (III) acetyl-acetonate
‡‡ RE solution: 7 = Erbium (III) acetyl-acetonate
§§ RE solution: 8 = Ytterbium (III) acetyl-acetonate

Table 4.2 BET nitrogen single point surface area characterization results.

Sample No.	Name	Method	BET surface area (m^2/g)
Blank	KL	N/A	326.9
00	Pt/SiO_2	IWI	130.8
11	Pt/KL	IWI	224.9
12	Pt/Ce/KL	IWI	250.9
13	Pt/Er/KL	IWI	187.1
14	Pt/Yb/KL	IWI	191.4
21	Pt/KL	VPI	224.5
22	Pt/Ce/KL	VPI	277.5
23	Pt/Er/KL	VPI	242.7
24	Pt/Yb/KL	VPI	217.9

Table 4.3 Pore volume results characterized by BET surface area analysis.

Catalyst	Micro pore volume (cc./g.)
KL (Blank)	0.14660
Pt/KL	0.08632

Since the surface area of the zeolite without impregnated Pt, *i.e.*, blank KL, was much higher than those surface areas of supported catalysts, as shown in Table 4.2, the metal and/or promoter loading can reasonably cause a decline in BET surface area. For Pt/KL catalyst, KL zeolite was covered by platinum metal and hence decreasing in overall surface area. Pt/SiO_2, the amorphous form, had a lower surface area than those of Pt/KL catalysts. For a series of Pt/KL catalysts prepared by IWI method, Cerium promoter enhanced the surface area of Pt/KL catalysts. In contrast, Erbium and Ytterbium loadings gave unexpected decreases in surface areas. Pt/KL prepared by VPI method did not show a significant difference from that

prepared by IWI method. However, with loadings of rare earth (*e.g.*, Ce, Er, Yb) by VPI method provided more surface area for the samples than those prepared by IWI method. Data showing a decrease in pore volume when loading platinum on KL zeolite as seen in Table 4.3 confirmed the dispersion of platinum particle on Pt/KL zeolite.

4.2.2. Atomic Absorption Spectroscopy (AAS)

Table 4.4 Platinum wt% loading testing results characterized by AAS

Sample No.	Name	%Pt
00	Pt/SiO_2	0.44
11	Pt/KL	0.88
21	Pt/KL	0.84
22	Pt/Ce/KL	1.11
23	Pt/Er/KL	1.04
24	Pt/Yb/KL	1.01

Due to several problems, *e.g.*, standard solution, incomplete digesting, AAS results only showed the approximate %Pt in the catalysts. However, the results of all Pt loadings were approximately 1%, which corresponded to the desired value. In Pt/SiO_2, its obviously low observed Pt wt% loading suggested some different properties from those of Pt/KL, *e.g.*, the bonding between metal and support in Pt/SiO_2 catalyst perhaps was stronger than that bonding in Pt/KL. The promoters may somehow help the aqua regia to dissolve Pt from metal surface, *e.g.*, lowering the bond strength between platinum and support and/or decreasing the size of platinum clusters.

4.3. Reaction Testing

4.3.1. The Effect of Catalyst Types and Preparation Methods on C_1/C_3 Molar Ratio

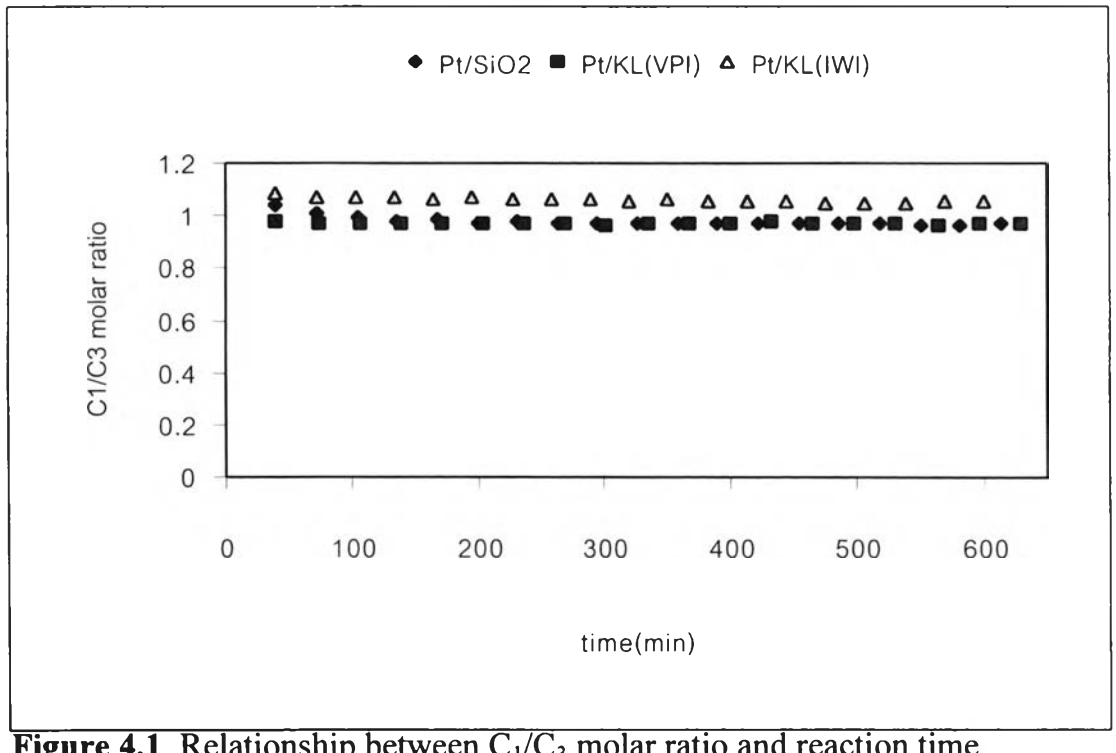

Figure 4.1 Relationship between C_1/C_3 molar ratio and reaction time of different catalyst types and preparation methods carried out at 350°C, HC : H_2 ~ 1 : 10.

According to n-butane hydrogenolysis stoichiometry, methane generated rate would be equal to propane generated rate if no further cracking occured. Therefore C_1/C_3 molar ratio would be unity. In accordance with Figure 4.1, C_1/C_3 molar ratios of both Pt/SiO_2 and Pt/KL (both prepared by IWI and VPI) were nearly unity as expected. These results indicated that only single hydrogenolysis occurred (no further cracking occurred).

4.3.2. The Effect of Catalyst Types and Preparation Methods on C_2/C_1 Molar Ratio

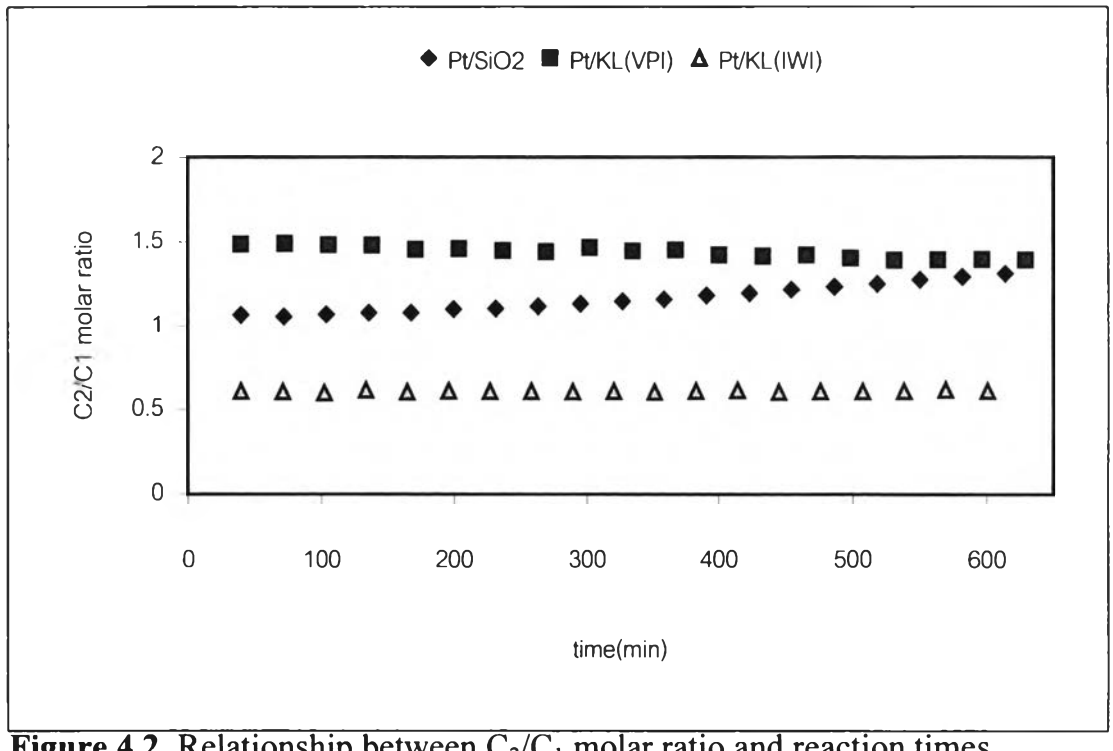

Figure 4.2 Relationship between C_2/C_1 molar ratio and reaction times of different catalyst types and preparation methods carried out at 350°C, HC : H_2 ~ 1 : 10.

The value of F is defined as the probability of breaking the central C-C bond in n-butane molecules. C_2/C_1 molar ratios for Pt/KL prepared by VPI method were around 1.5, hence, the possible probability of breaking the central C-C bond in n-butane molecule (F) was around 0.43 (See Appendix A). In the first period, C_2/C_1 molar ratios for Pt/SiO_2 indicated the same probability of breaking any C-C bond in butane molecule (See Appendix A). Increasing in C_2/C_1 molar ratio (See Figure 4.2) and decreasing in conversion with time (See Figure 4.3) indicated the decreasing of terminal C-C bond splitting. The explanation is that when conversion decreased, methane, ethane, and propane mole fractions commonly decreased. However, the C_2/C_1 molar ratio increased when time increased (See Figure 4.2).

Therefore the possible decreasing of terminal C-C bond splitting was proposed. Pt/KL prepared by IWI showed the lowest value of F (See Figure 4.2 & Appendix A). This may be because of the large platinum clusters left outside the channels of the zeolite. Since the high C_2/C_1 molar ratio from Pt/KL (VPI) having small platinum particle size was observed, one conclusion may be that the small size of platinum particle located uniformly inside the channels of the zeolite was the contributory factor to enhancing the probability of breaking the central C-C bond in n-butane molecule.

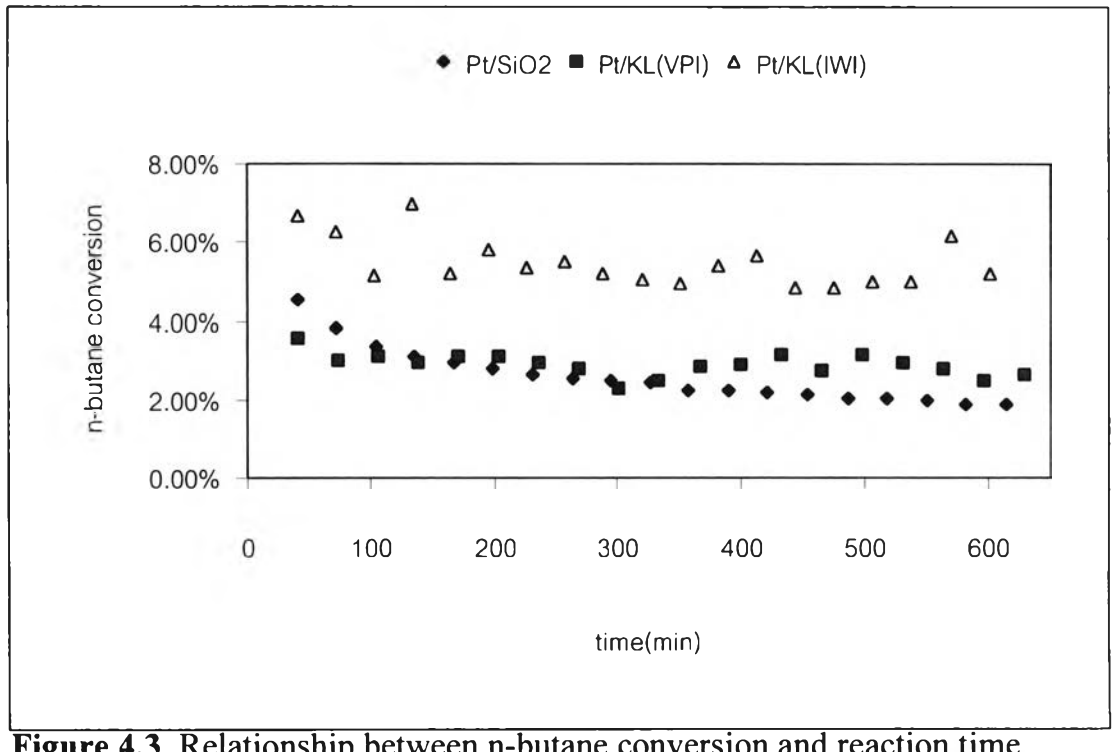

Figure 4.3 Relationship between n-butane conversion and reaction time of different catalyst types and preparation methods carried out at 350°C, HC : H_2 ~ 1 : 10.

4.3.3. The Effect of Promoters on C_1/C_3 Molar Ratio

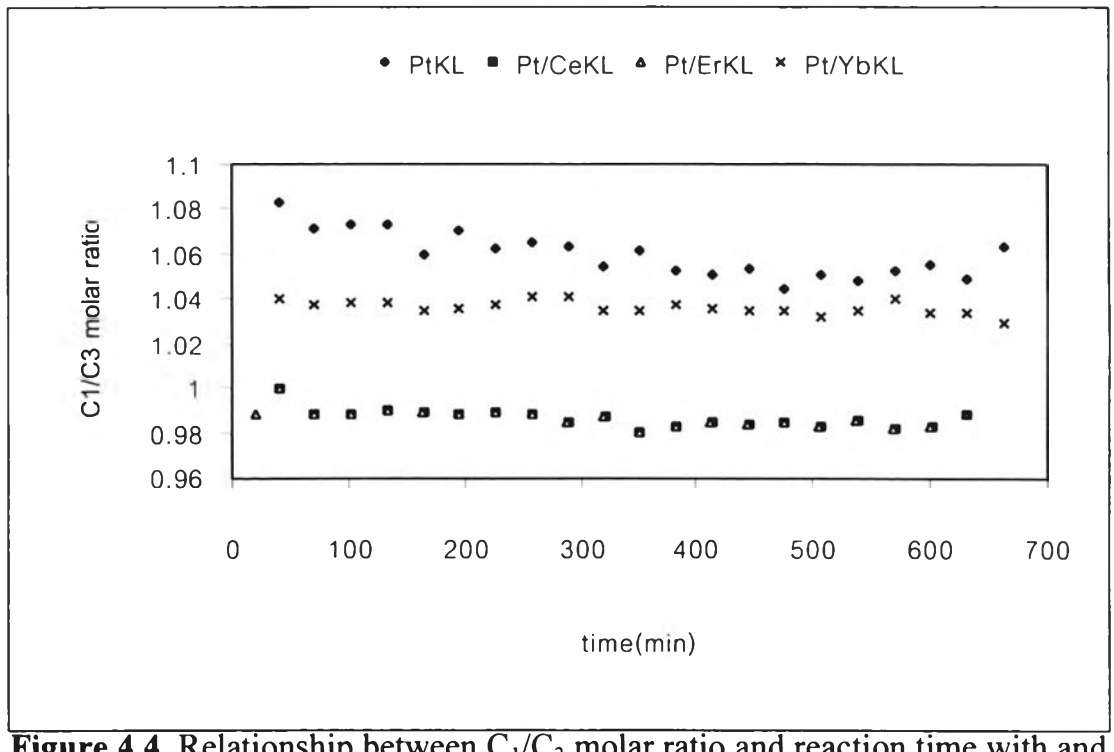

Figure 4.4 Relationship between C_1/C_3 molar ratio and reaction time with and without promoters carried out at 350°C, HC : H_2 ~ 1 : 10.

C_1/C_3 molar ratios of the unpromoted catalyst, which were slightly higher than those of the promoted catalysts, indicated the strong adsorption of C_3 species formed from the reaction. Hence, further cracking occurred more easily and resulted in higher C_1/C_3 molar ratio than those observed from the promoted catalysts as shown in Figure 4.4. The data shown in Figure 4.4 reinforce the 2,3-diadsorbed mechanism proposed by Bond and Lin (1997) as shown in Figure 4.5. Since promoters promoted the formation of 2,3-diadsorbed butane, C_3 species were formed more difficultly on the promoted catalyst. Hence, deep hydrogenolysis occurred more difficultly on the promoted catalysts. In other words, deep hydrogenolysis occurred more easily on the unpromoted catalyst, resulting in slightly higher C_1/C_3 molar ratio. However, only partial deep hydrogenolysis occurred at 350°C, therefore,

both the unpromoted catalyst and the promoted catalysts showed C_1/C_3 molar ratio of nearly unity.

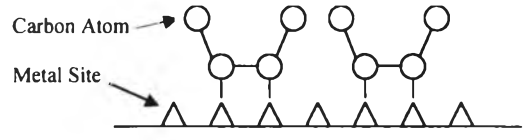

Figure 4.5 The 2,3-diadsorption mechanism of n-butane hydrogenolysis proposed by Bond and Lin (1997).

4.3.4. The Effect of Promoters on C_2/C_1 Molar Ratio

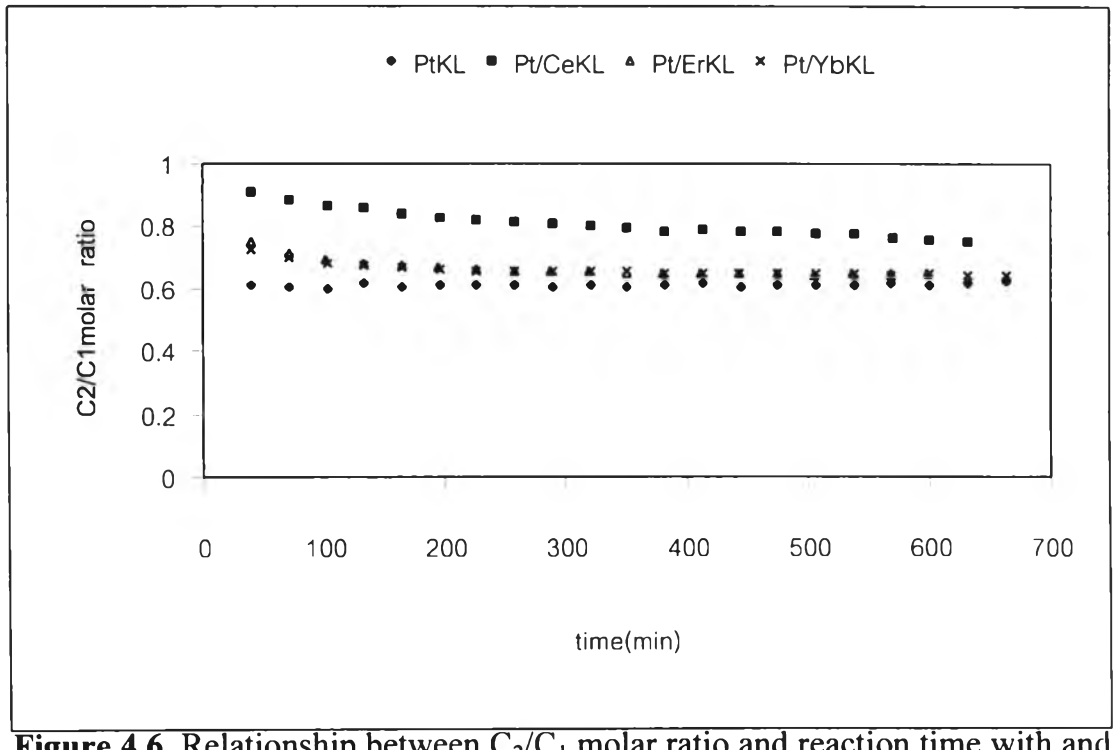

Figure 4.6 Relationship between C_2/C_1 molar ratio and reaction time with and without promoters carried out at 350°C, HC : H_2 ~ 1 : 10.

From Figure 4.6, C_2/C_1 molar ratio of the unpromoted catalyst was the lowest. These observations suggested that the promoters differently increase the F value of the Pt/KL catalysts. The explanation is that the promoters inhibit the agglomeration of platinum clusters, which leads to enhancing the metal dispersion of the catalyst and achieving small platinum particle size; hence, elevate the F value.

4.3.5. The Effect of Temperatures on C_1/C_3 Molar Ratio

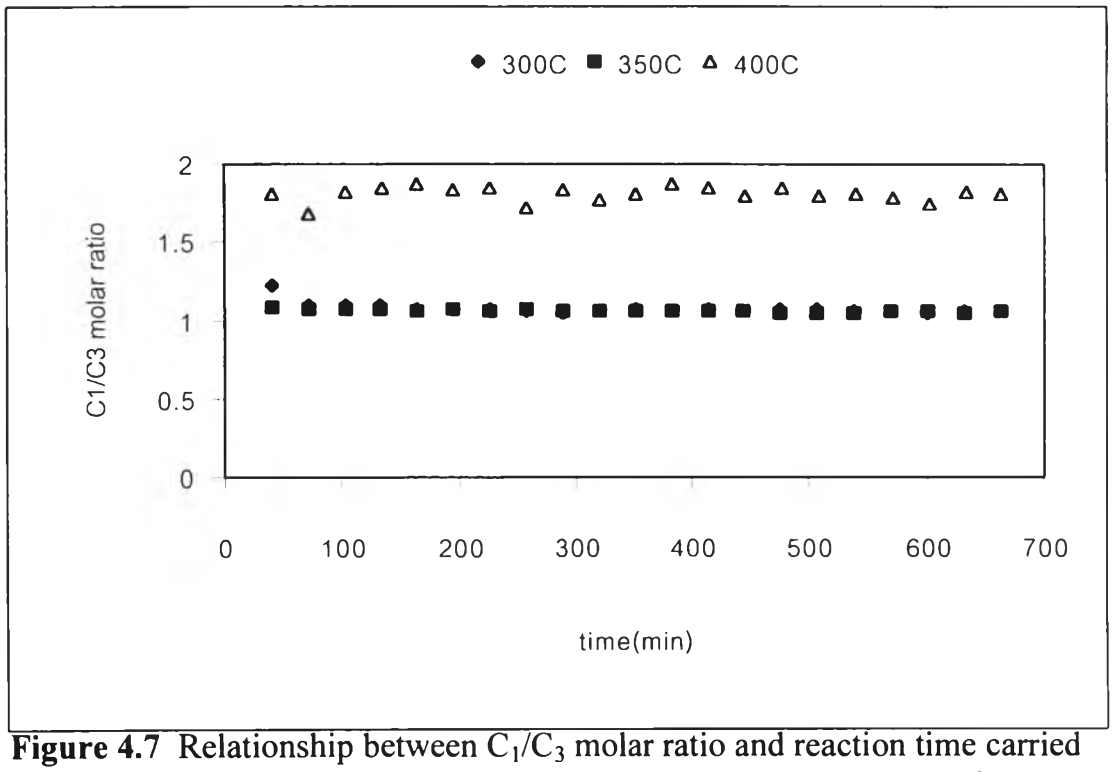

Figure 4.7 Relationship between C_1/C_3 molar ratio and reaction time carried out on Pt/KL (IWI) catalyst at different temperatures, HC : H_2 ~ 1 : 10.

From Figure 4.7, C_1/C_3 molar ratio results affected by different reaction temperatures indicated different hydrogenolysis. At low temperatures (300 and 350°C), low conversion was obtained (See Figure E3, Appendix E) and one of C-C bonds in butane molecule splitted once and desorbed. At higher temperature (400°C), higher conversion was obtained

(See Figure E3, Appendix E) and the substantially high C_1/C_3 molar ratio results indicated that deep hydrogenolysis did occured.

4.3.6. The Effect of Temperatures on C_2/C_1 Molar Ratio

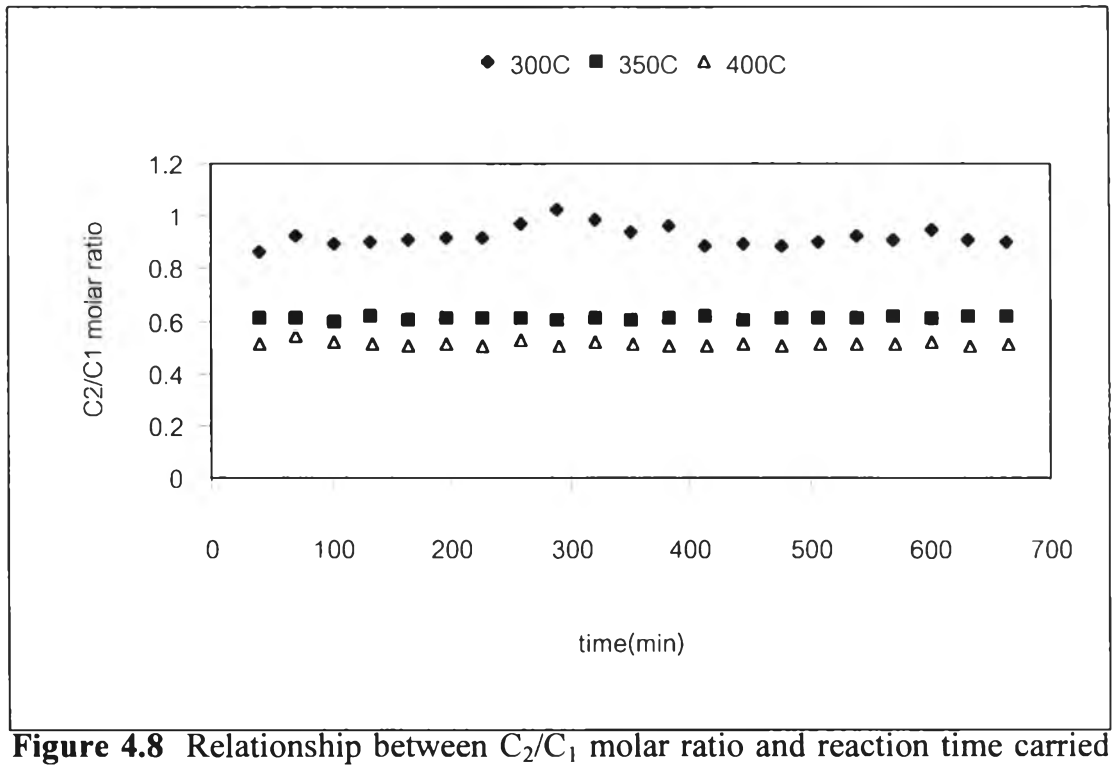

Figure 4.8 Relationship between C_2/C_1 molar ratio and reaction time carried out on Pt/KL (IWI) catalyst at different temperatures, HC : H_2 ~ 1 : 10.

At 300°C, the conversions were very low (See Figure E3, Appendix E) and each C-C bond had nearly the same probability to be broken since C_2/C_1 molar ratios were nearly unity (See Appendix A). Due to the deep hydrogenolysis which occurred more at higher temperatures, C_2/C_1 molar ratios decreased from those ratio at 350°C to approximately 0.5 at 400°C, which was still higher than the expected value (~ 0.3-0.4). The explanation is that the deep hydrogenolysis increased both C_1 and C_2 mole fractions, led to higher C_2/C_1 molar ratio than the expected value (~ 0.3-0.4). As a result, C_2/C_1 ratios at 400°C were closed to those ratios at 350°C. C_2/C_1 ratios at 300°C were nearly unity, hence, the values of F were closed to 0.33 (See Appendix A). Since C_2/C_1 ratios at 350°C were 0.6, the values of F were

around 0.23 (See Appendix A). F value results indicated that the probability of breaking the terminal C-C bond at 350°C was lower than that at 300°C. At 400°C, deep hydrogenolysis made F value evaluation much more complicated. When deep hydrogenolysis becomes important, methane, ethane, and propane mole fractions were affected by the further cracking of the adsorbed C_3 species. As a result, the F value can not be calculated directly from the observed C_2/C_1 molar ratio results. In accordance with the results shown in Figure 4.8, the higher the reaction temperature, the lower the probability of central C-C bond breaking.

4.3.7. The Effect on Isobutane Selectivity

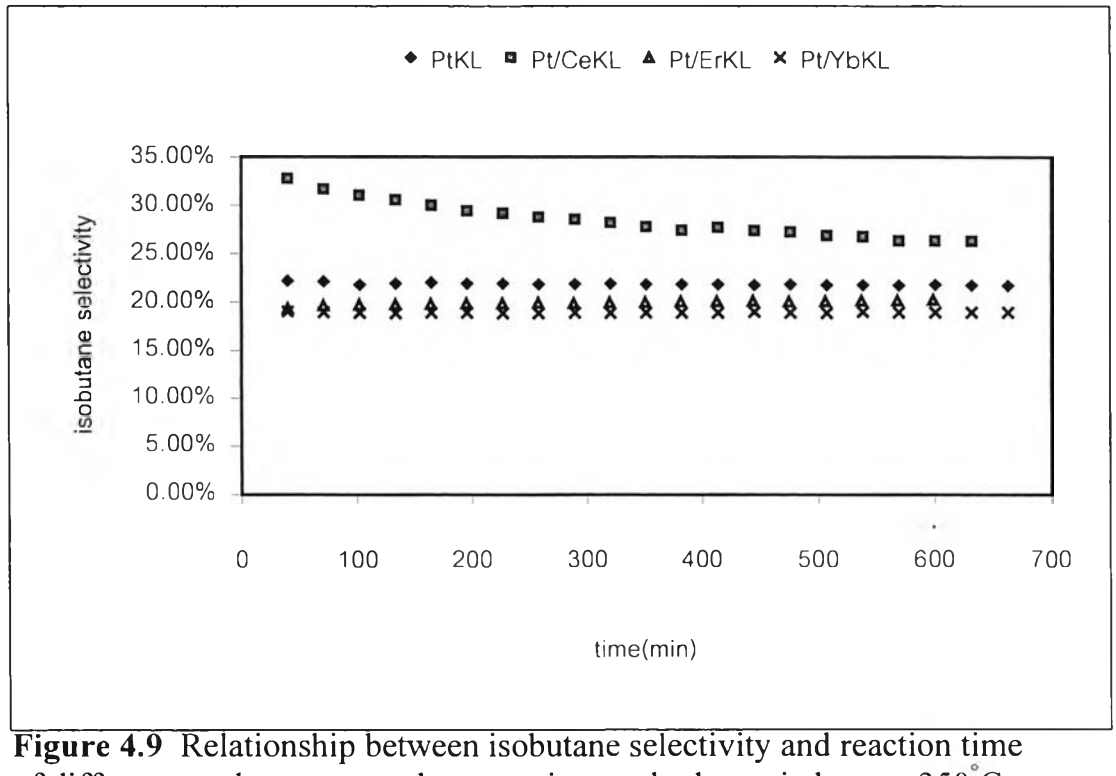

Figure 4.9 Relationship between isobutane selectivity and reaction time of different catalyst types and preparation methods carried out at 350°C, HC : H_2 ~ 1 : 10.

The amorphous Pt/SiO_2 catalyst showed high isobutane selectivity as seen in Figure 4.9. However, it also showed a dramatically decrease in isobutane selectivity once the coverage increased with time. At low coverage, isobutane may be formed easily, resulting in high isobutane selectivity. In the ensuing period, with higher coverage, the steric effect of branched group in isobutane structure played more important role. The formation of new isobutane molecules may be obstructed by the neighboring adsorbed isobutane molecules previously formed, leading to the decreasing in isobutane selectivity until the equilibrium was established. In contrast to the supported silica catalyst, the supported KL catalysts gave significantly low isobutane selectivity probably due to the linear channels structure of KL zeolite (See Figure 4.9). Some large platinum cluster located outside the channels of KL zeolite, found in the catalysts prepared by IWI method, led to slightly higher isobutane selectivities than those observed in the catalysts prepared by VPI method. The explanation is that the platinum clusters located outside the pore acted similarly to those platinum particles on the silica.

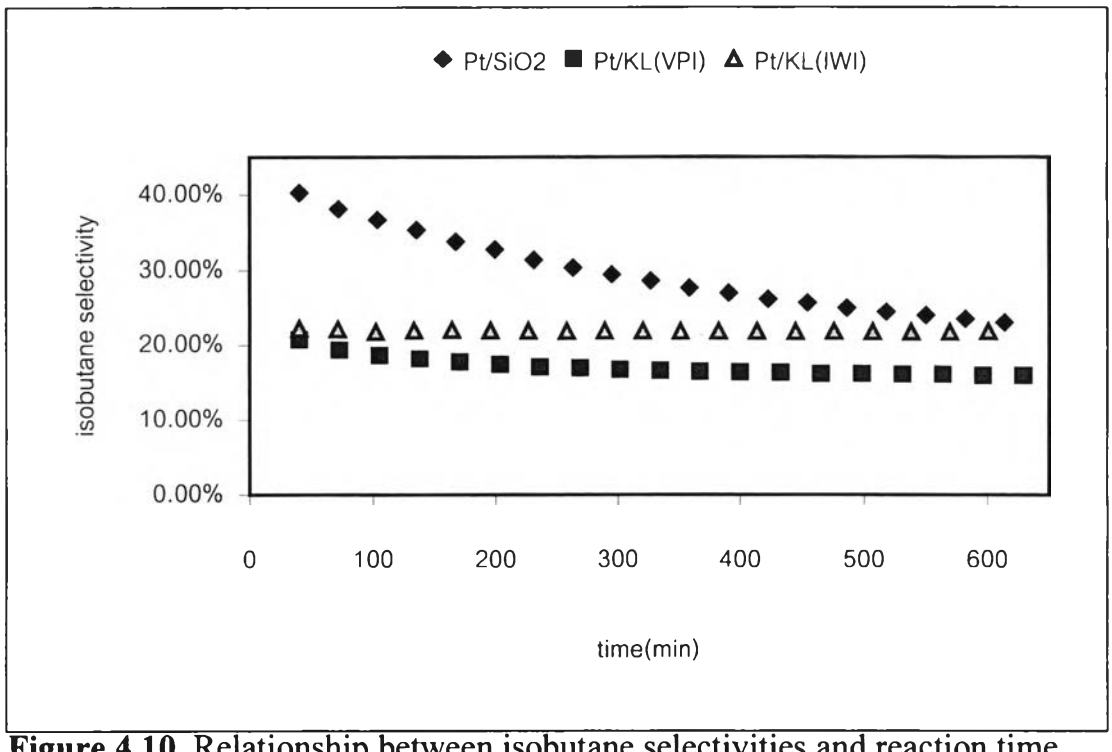

Figure 4.10 Relationship between isobutane selectivities and reaction time with and without promoters carried out at 350°C, HC : H_2 ~ 1 : 10.

From Figure 4.10, the promoters did not play a momentous role on isobutane selectivity except for cerium, which promoted isomerization. It may be that Ce gave the highest metal dispersion, led to small platinum particle size, and favored the formation of 2,3-diadsorbed n-butane. Therefore the Ce promoted Pt/KL catalyst showed the highest isobutne selectivity.

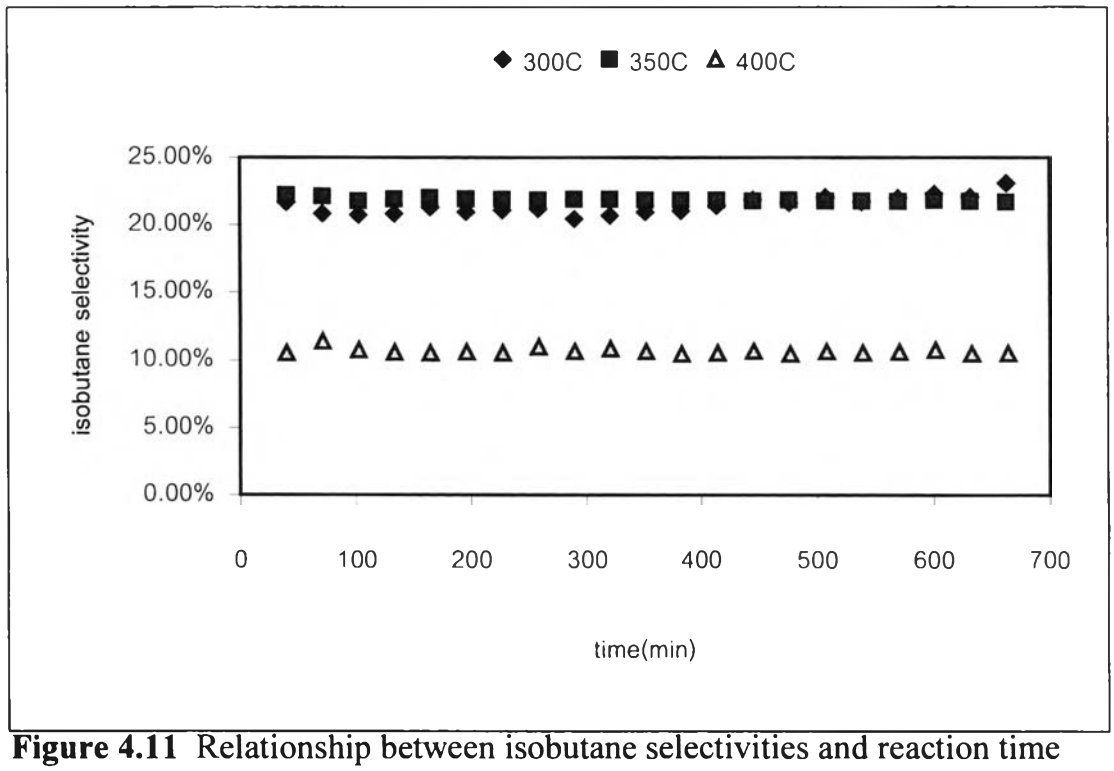

Figure 4.11 Relationship between isobutane selectivities and reaction time carried out on Pt/KL (IWI) catalyst at different temperatures, HC : H_2 ~ 1 : 10.

From figure 4.11, the isobutane selectivity at 300 and 350°C were about the same. On the other hand, at 400°C, deep hydrogenolysis occurred. This gave higher methane, ethane, and propane mole fractions than at lower reaction temperatures, resulting in much lower isobutane selectivity (See Figure 4.11).

4.3.8 The Effect of Hydrogen Pressure on the Reaction Rates

The dependence of the reaction rates on H_2 pressure was studied under the method of fixed hydrocarbon pressure and varied hydrogen pressure at 350, 375, and 400°C. Due to the strong adsorption of hydrogen reported by Bond (1997), the decrease of reaction rates with increasing hydrogen pressure was found at 375 and 400°C (See Table 4.6 & 4.7). However, the unusual change in the reaction rate was obtained at 350°C (See Table 4.5) and the change was in the opposite direction. The hydrogen orders

were calculated using Equation 4.1. The hydrogen orders ranged from 1.7 to 2.1 at 350°C, -1 to -0.6 at 375°C, and -1.7 to -1.2 at 400°C. These fluctuations of the orders may be caused by the unstable flow rates, which led to the change in system pressure during the reaction.

4.3.9 The Effect of Hydrocarbon Pressure on the Reaction Rates

The effects of hydrocarbon pressure on the reaction rates were studied under the method of fixed hydrogen pressure and varied hydrocarbon pressure at 350, 375, and 400°C. The reaction rates were proportional to hydrocarbon pressure at the temperatures between 350 to 400°C. The hydrocarbon orders were calculated base on Equation 4.1. The hydrocarbon orders were 0.6 to 1.6 at 350°C, 0.6 to 1.4 at 375°C, and 2 to 2.9 at 400°C.

Table 4.5 The dependence of the reaction rates on hydrogen and hydrocarbon pressure at 258 minute, 350°C.

P_{H2} (kPa)	Rate (mmol/h·gcat)	P_{HC} (kPa)
44.1390	0.0195	7.4908
75.8117	0.0501	7.4908
75.8117	0.0790	11.8830

Table 4.6 The dependence of the reaction rates on hydrogen and hydrocarbon pressure at 258 minute, 375°C.

P_{H2} (kPa)	Rate (mmol/h·gcat)	P_{HC} (kPa)
39.6519	0.1042	8.0402
74.7224	0.0568	8.0402
74.7224	0.0783	10.2319

Table 4.7 The dependence of the reaction rates on hydrogen and hydrocarbon pressure at 258 minute, 400°C.

P_{H2} (kPa)	Rate (mmol/h·gcat)	P_{HC} (kPa)
37.5751	0.2265	6.3656
70.9423	0.0793	6.3656
70.9423	0.3223	10.3019

$$r = kP_{HC}^{\alpha} P_{H2}^{\beta} \quad (4.1)^{*}$$

$$r = \frac{k_0 e^{-E/RT} K_{HC0} e^{\Delta H_{HC}/RT} K_{H20} e^{\Delta H_{H2}/RT} P_{HC} P_{H2}}{\left(1 + K_{HC0} e^{\Delta H_{HC}/RT} P_{HC} + K_{H20} e^{\Delta H_{H2}/RT} P_{H2}\right)^2} \quad (4.2)^{\dagger}$$

4.3.10 Activation Energy

The calculated apparent activation energies changed with increasing or decreasing of hydrocarbon or hydrogen partial pressure as shown in Table 4.8, which corresponded to the Langmuir-Hinshelwood kinetics (See Equation 4.2). Moreover, Van de Runstraat *et al.* (1997) reported that the surface coverage is one main reason for the change in the apparent activation energy. However, the true activation energy does not depend on pressures. At 350 to 400°C, the Arrhenius plot showed that the activation energy did not depend on temperature (See Figure 4.12).

According to the calculation results shown in Table 4.8, the increasing of hydrogen pressure could decrease the activation energy. This may be because the large amount of H_2 can cause high value of ΔH_{ads}, and therefore, the apparent activation energy was decreased. Hydrocarbon pressure was proportional to the activation energy. It may be explained that

---

* See Appendix B

† Langmuir-Hinshelwood kinetics, See Appendix D

due to the less amount of HC in the feed stream, ΔH_{ads} did not significantly affect the apparent activation energy. However, the change in the apparent activation energy with hydrocarbon pressure can be explained by the formation of adsorbed n-butane molecules, as shown in Figure 4.13 & 4.14. At low hydrocarbon pressure (See Figure 4.13), di-adsorption was more easily formed, hence, the C-C bond was easier to crack, and therefore, the activation energy decreased. At high hydrocarbon pressure (See Figure 4.14), the mono-adsorption is favored, hence, the C-C bond was more difficult to crack, and therefore, the activation energy increased.

Table 4.8 The dependence of activation energy on hydrogen and hydrocarbon pressure at 258 minute.

P_{H2} (kPa)	Ea (kJ/mol)	P_{HC} (kPa)
73.42	113.16	10.80
73.42	50.08	7.30
40.46	176.64	7.30

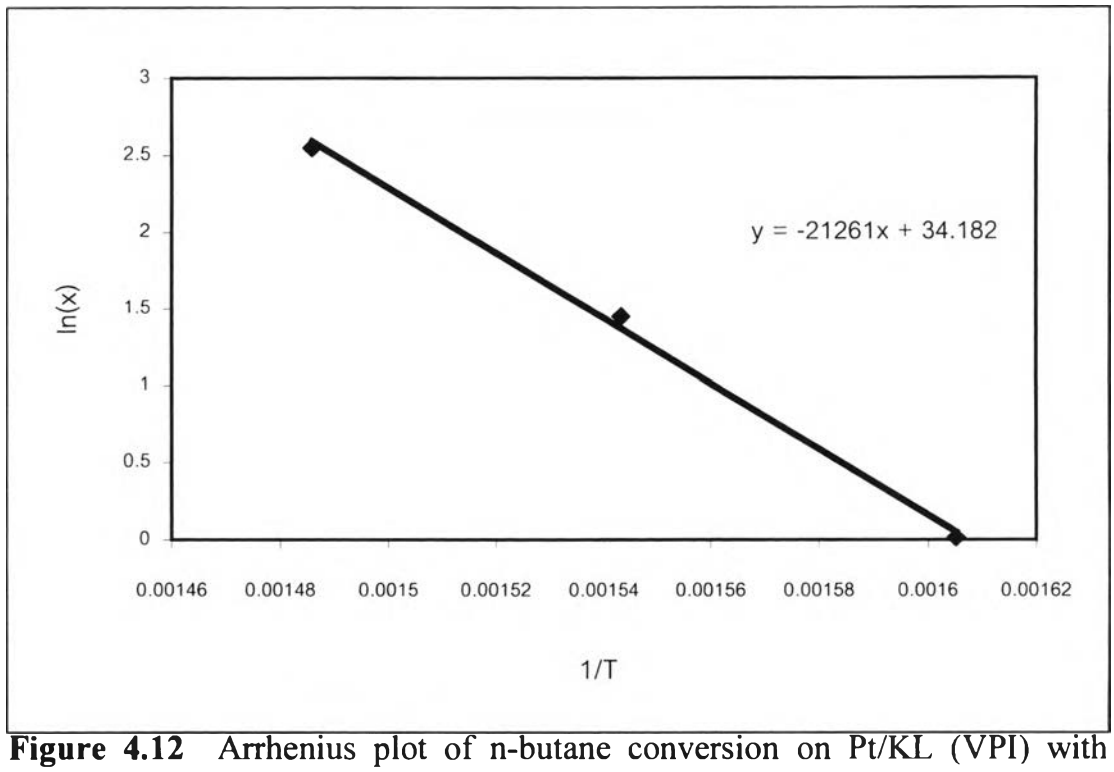

Figure 4.12 Arrhenius plot of n-butane conversion on Pt/KL (VPI) with P_{H2} = 40.46 kPa and P_{HC} = 7.30 kPa at 258 minute.

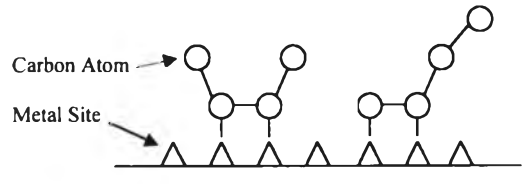

Figure 4.13 The adsorption model of n-butane molecule at low hydrocarbon (*i.e.*, n-butane) pressure.

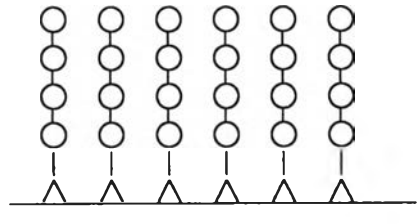

Figure 4.14 The adsorption model of n-butane molecule at high hydrocarbon (*i.e.*, n-butane) pressure.